X-Ray Spectral Properties of Low-Mass X-Ray Binaries in Nearby Galaxies

Jimmy A. Irwin – University of Michigan
Alex E. Athey – University of Michigan
Joel N. Bregman – University of Michigan

Citation of published version:

Irwin, J., Athey, A., Bregman, J. (2003): X-Ray Spectral Properties of Low-Mass X-Ray Binaries in Nearby Galaxies. *The Astrophysical Journal*, 587(1). DOI: 10.1086/368179

The Astrophysical Journal, 587:356–366, 2003 April 10

X-RAY SPECTRAL PROPERTIES OF LOW-MASS X-RAY BINARIES IN NEARBY GALAXIES

Jimmy A. Irwin,[1,2] Alex E. Athey,[1] and Joel N. Bregman[1]

Received 2002 September 3; accepted 2002 December 20

ABSTRACT

We have investigated the X-ray spectral properties of a collection of low-mass X-ray binaries (LMXBs) within a sample of 15 nearby early-type galaxies using proprietary and archival data from the *Chandra X-Ray Observatory*. We find that the spectrum of the sum of the sources in a given galaxy is remarkably similar from galaxy to galaxy when only sources with X-ray luminosities less than 10^{39} ergs s^{-1} (0.3–10 keV) are considered. Fitting these lower luminosity sources in all galaxies simultaneously with a power-law model led to a best-fit power-law exponent of $\Gamma = 1.56 \pm 0.02$ (90% confidence), and using a thermal bremsstrahlung model yielded $kT_{\rm brem} = 7.3 \pm 0.3$ keV. This is the tightest constraint to date on the spectral properties of LMXBs in external galaxies. The spectral properties of the LMXBs do not vary with galactic radius out to three effective radii. There is also no apparent difference between the spectral properties of LMXBs that reside within globular clusters and those that do not. We demonstrate how the uniformity of the spectral properties of LMXBs can lead to more accurate determinations of the temperature and metallicity of the hot gas in galaxies that have comparable amounts of X-ray emission from hot gas and LMXBs. Although few in number in any given galaxy, sources with luminosities of (1–2) $\times$ 10^{39} ergs s^{-1} are present in 10 of the galaxies. The spectra of these luminous sources are softer than the spectra of the rest of the sources and are consistent with the spectra of Galactic black hole X-ray binary candidates when they are in their very high state. The spatial distribution of these sources is much flatter than the optical light distribution, suggesting that a significant portion of them must reside within globular clusters. The simplest explanation of these sources is that they are $\sim$10–15 $M_{\odot}$ black holes accreting near their Eddington limit. The spectra of these sources are very different from those of ultraluminous X-ray sources (ULXs) that have been found within spiral galaxies, suggesting that the two populations of X-ray–luminous objects have different formation mechanisms. The number of sources with apparent luminosities above 2×10^{39} ergs s^{-1} when determined using the distance of the galaxy is equal to the number of expected background active galactic nuclei and thus appears not to be associated with the galaxy, indicating that very luminous sources are absent or very rare in early-type galaxies. The lack of ULXs within elliptical galaxies strengthens the argument that ULXs are associated with recent star formation.

Subject headings: binaries: close — X-rays: galaxies — X-rays: stars

On-line material: color figure

1. INTRODUCTION

The *Chandra X-Ray Observatory* has made it possible to resolve dozens if not hundreds of individual X-ray point sources in nearby galaxies owing to its subarcsecond spatial resolution (Sarazin, Irwin, & Bregman 2000; Angelini, Loewenstein, & Mushotzky 2001; Kraft et al. 2001; Bauer et al. 2001; Soria & Wu 2002). While spiral galaxies contain a variety of types of X-ray point sources (high- and low-mass X-ray binaries, supernova remnants), elliptical and S0 galaxies, as well as the bulges of spiral galaxies, contain almost exclusively low-mass X-ray binaries (LMXBs). LMXBs are believed to be composed of a compact accreting primary (a neutron star or a black hole) and a low-mass main-sequence or red giant secondary that is losing material to the primary as a result of Roche lobe overflow. Although LMXBs have been studied extensively in our Galaxy, resolving them and determining their spatial distribution and spectral characteristics in external galaxies has only recently become feasible.

Initial work on the LMXB population of early-type galaxies has led to several interesting results. Sarazin, Irwin, & Bregman (2000, 2001) detected 90 X-ray sources in a *Chandra* observation of the elliptical galaxy NGC 4697 and found a break in the luminosity function of the sources at a luminosity of $\sim 3 \times 10^{38}$ ergs s^{-1}, intriguingly close to the Eddington luminosity of an accreting 1.4 $M_{\odot}$ neutron star. One interpretation of this break is that it represents a division between black hole X-ray binaries and neutron star X-ray binaries, with only black hole binaries more luminous than the break and a mixture of neutron star and black hole binaries less luminous than the break. Such breaks have also been found in other early-type galaxies (Blanton, Sarazin, & Irwin 2001; Finoguenov & Jones 2002; Randall, Sarazin, & Irwin 2002; Kundu, Maccarone, & Zepf 2002). Recent studies have also found that a significant fraction (40%–70%) of the X-ray binaries reside in globular clusters of the host galaxy (Angelini et al. 2001; Randall et al. 2002; Kundu et al. 2002), in marked contrast to the $\sim$10% of Galactic and M31 LMXBs that reside within globular clusters. In addition, when the spectra of all the resolved LMXBs of a given galaxy were added together and fitted with a power-law spectral model, an index ranging from 1.5 to 2.0 was obtained (Sarazin et al. 2001; Randall et al. 2002; Kim & Fabbiano 2003; Irwin, Sarazin, & Bregman 2002).

[1] Department of Astronomy, University of Michigan, Ann Arbor, MI 48109-1090; jirwin@astro.lsa.umich.edu, aathey@umich.edu, jbregman@umich.edu.

[2] *Chandra* Fellow.

Previous X-ray satellites lacked the needed spatial resolution and bandpass coverage to separate cleanly the LMXB component from the hot gas component in early-type galaxies. While recent progress has been made from the study of the luminosity functions and host environment of LMXBs in early-type galaxies, a detailed analysis of the spectral properties of LMXBs with a large sample of galaxies has not yet been attempted with *Chandra*. With *Chandra* we are now in a position to determine the spectral properties of individual bright sources in galaxies or add up the spectra of the fainter sources to determine the bulk spectral properties of the LMXBs.

A more thorough understanding of the X-ray spectral properties of LMXBs in early-type galaxies is critical for the study of the hot, X-ray–emitting gas within these systems. Although the LMXB contribution to the X-ray emission from gas-rich galaxies is negligible, this is not the case for galaxies with moderate to low amounts of X-ray–emitting gas. In these galaxies, the LMXB contribution can be the dominant X-ray emission mechanism. Quantifying the spectral properties of LMXBs in nearby galaxies where the LMXBs are resolvable will allow for a more accurate separation of the gaseous and stellar X-ray components in galaxies too distant for the individual LMXBs to be detected.

In this paper we use both proprietary and archival *Chandra* data for 15 early-type systems (consisting of eight elliptical galaxies, two transitional E/S0 galaxies, three S0 galaxies, and two spiral bulges) to determine the spectral characteristics of LMXBs over a range of X-ray luminosity classes, as well as a function of galactic radius. Unless otherwise stated, all uncertainties are 90% confidence levels, and all X-ray luminosities are in the 0.3–10 keV energy band.

2. OBSERVATIONS AND DATA REDUCTION

We have constructed a sample of 13 early-type galaxies and two spiral bulges that were observed with the ACIS S3 chip on board *Chandra*. The sample is given in Table 1. The assumed distances were taken from Tonry et al. (2001) with the exceptions of NGC 1291 (de Vaucouleurs 1975) and M31 (van den Bergh 2000), and the assumed Galactic hydrogen column densities are from Dickey & Lockman (1990).

The galaxies in the sample were processed in a uniform manner following the *Chandra* data reduction threads employing CIAO 2.2.1 coupled with CALDB 2.12. All of the data were calibrated with the most recent gain maps at the time of reduction (acisD2000-08-12gainN0003.fits for -120°C focal plane temperature data and acisD2000-08-12gainN0003.fits for -110°C data). *ASCA* grades of 0, 2, 3, 4, and 6 were selected for all subsequent processing and analysis. The observation-specific bad pixel files were applied from the standard calibration library included with CIAO 2.2.1. Pileup was not an issue even for the brightest sources, and no correction has been applied.

To check for background flares, a temporal light curve was constructed from the outer regions of the ACIS S3 chip. We examined each light curve by eye and eliminated any data approximately 3–4 σ away from a determined mean value during a quiescent period. Typically, this eliminated less than 15% of the data. Since our goal is to detect point sources rather than diffuse emission, strict screening of high background rates is not necessary. The peak of the energy distribution of the source region was determined and used to generate an exposure map appropriate for that energy for each observation. Sources were detected using the "Mexican hat" wavelet detection routine *wavdetect* in CIAO in an 0.3–6.0 keV band image. The threshold was set to give approximately one false detection per image, and the scales run were from 2 to 32 pixels. The source list of each galaxy was culled to remove any source not detected at the 3 σ level.

In order to reduce contamination from unrelated foreground/background X-ray sources, we restrict our study to sources within three effective (half-optical light) radii of the center of each galaxy. Effective semimajor and semiminor axes as well as position angles were collected from the literature (see Table 1). In galaxies with large amounts of hot, diffuse gas (i.e., NGC 1399, NGC 4472), some sources

TABLE 1
SAMPLE OF GALAXIES

Galaxy Number	Galaxy	Type	Observation ID	Distance (Mpc)	Semimajor Axis (arcsec)	Semiminor Axis (arcsec)	Axis Reference	N_H ($\times 10^{20}$ cm^{-2})	Exposure (s)	Luminosity Limit (ergs s^{-1})
1	NGC 1291	Sa	795	8.9	...	...	...	2.12	37,406	2.0×10^{37}
2	NGC 1316	S0	2022	21.5	132.2	90.5	1	1.88	24,478	1.7×10^{38}
3	NGC 1399	E1	319	20.0	44.6	40.5	2	1.34	54,540	6.4×10^{37}
4	NGC 1407	E0	791	28.8	73.9	68.7	2	5.42	48,331	2.0×10^{38}
5	NGC 1549	E0	2077	19.7	51.0	44.7	2	1.46	24,468	1.7×10^{38}
6	NGC 1553	S0	783	18.5	78	51	3	1.50	28,168	1.1×10^{38}
7	NGC 3115	S0	2040	9.7	93	35	4	4.32	36,979	2.9×10^{37}
8	NGC 3585	E/S0	2078	20.0	56	28	5	5.57	33,706	1.6×10^{38}
9	NGC 4374	E1	803	18.4	58.2	53.3	2	2.60	28,049	9.8×10^{37}
10	NGC 4472	E2	321	16.3	114.0	95.6	6	1.66	38,598	7.0×10^{37}
11	NGC 4494	E1	2079	17.1	49.3	42.2	2	1.52	22,974	1.1×10^{38}
12	NGC 4636	E/S0	323	14.7	117.0	85.6	6	1.81	50,544	4.2×10^{37}
13	NGC 4649	E2	785	16.8	82.0	66.2	6	2.20	35,923	7.7×10^{37}
14	NGC 4697	E6	784	11.8	97.3	60.2	2	2.12	39,063	3.2×10^{37}
15	M31	Sb	309	0.76	...	...	...	6.66	5,089	1.2×10^{36}

REFERENCES.—(1) Caon, Capaccioli, & D'Onofrio 1994; (2) Goudfrooij et al. 1994; (3) Kormendy 1984 and Jorgensen, Franx, & Kjaergaard 1995; (4) Capaccioli, Held, & Nieto 1987; (5) Ryden, Forbes, & Terlevich 2001; (6) Peletier et al. 1990.

near the center of the galaxy were omitted since their count rates were highly uncertain owing to the presence of the high X-ray surface brightness gas.

For each source a local background was determined from a circular annular region with an inner radius that was set to 1.5 times the semimajor axis of the source extraction region and an outer radius chosen such that the area of the background annulus was 5 times the area of the source's extraction region. Care was taken to exclude neighboring sources from the background annuli of each source in crowded regions. We excluded point sources located at the optical center of each galaxy since it is likely that many of these sources are actually low-luminosity active galactic nuclei (AGNs) rather than LMXBs.

3. SPECTRAL ANALYSIS

For each galaxy, the spectra of all the sources in the galaxy within three effective radii were extracted and summed into one spectrum using the CIAO routine *acisspec*. This routine calculates a weighted redistribution matrix file (RMF) and ancillary response file (ARF) appropriate for extended sources or, for our case, a collection of point sources spread out over the ACIS detector. The ARF files have been corrected for the continuous degradation of the ACIS quantum efficiency[3] using the CIAO tool *corrarf*, which applies the ACISABS absorption profile (G. Chartas & K. Getman 2002[4]) to the original ARF file. The composite spectrum was then regrouped such that each energy channel contained at least 25 X-ray counts. Channels with energies less than 0.5 keV and greater than 6.0 keV were then excluded. The composite spectrum for each galaxy was then fitted within XSPEC Version 11.2.0 with a simple power-law model absorbed by the Galactic hydrogen column density (Table 1).

The results of these fits are shown in Figure 1 for each of the 15 galaxies in our sample. The best-fit power-law exponent varies from 1.45 to 1.9 from galaxy to galaxy, in agreement with previous *Chandra* studies of LMXBs in early-type systems. In general, freeing the absorption column density did not improve the quality of the fits, so the column densities have remained fixed at the Galactic value throughout the remainder of this paper. For the individual sources in each particular galaxy, the best-fit power-law exponent for that galaxy was used to convert the source count rates into 0.3–10 keV luminosities. The correction for the degradation of the ACIS quantum efficiency typically increased the power-law exponent by 10%–20% over the uncorrected value, with the correction greatest for the most recently observed targets, as is expected for linearly increasing absorption over time from molecular contamination of the ACIS optical blocking filters.

Next, we generated color-color plots for the individual sources in each galaxy. We define three X-ray bands, S (0.3–1.0 keV), M (1.0–2.0 keV), and H (2.0–6.0 keV), and create two X-ray colors, $H21 = (M - S)/(M + S)$ and $H31 = (H - S)/(H + S)$. The color-color plots of the 15 galaxies in our sample made it apparent that the most luminous sources ($L_X > 10^{39}$ ergs s^{-1}) tend to have significantly softer colors than the rest of the sources. This is illustrated

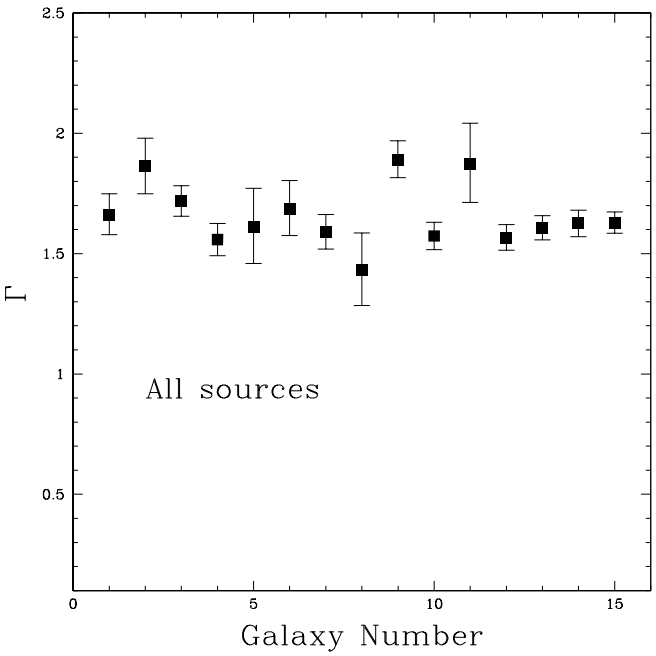

FIG. 1.—Best-fit power-law exponent (Γ) when the spectra of the sources were summed for each galaxy in our sample. The galaxy number corresponds to the numbering system in Table 1.

in Figure 2, where the H21 versus H31 values have been plotted for the sources within all the galaxies except NGC 1407, NGC 3115, NGC 3585, and M31, which have higher Galactic column densities that will artificially harden the colors. It is clear that the most luminous sources are indeed softer on average than the less luminous sources. We have performed a two-dimensional Kolmogorov-Smirnov test on the faint and bright sources and found that the probability that the H21 and H31 colors of the two distributions were chosen from the same parent distribution was only 0.004.

Also note the presence of a small number of sources at $(-1, -1)$. These sources have no detectable emission above 1 keV and are most likely supersoft sources, such as those seen in the Milky Way and the disk of M31. The traditional explanation of these supersoft sources is that they are accreting white dwarfs burning hydrogen on their surface (van den Heuvel et al. 1992). However, the bolometric luminosity of such a supersoft in M81 far exceeds the Eddington limit for a 1.4 $M_\odot$ white dwarf, prompting Swartz et al. (2002) to postulate that these sources are intermediate-mass black holes (10^2–10^3 $M_\odot$) accreting at a few percent of their Eddington limit, rather than white dwarfs. The brighter supersoft sources in our sample have similar bolometric luminosities. However, the small number of these sources found in our sample combined with their low count rates in the 0.5–6 keV energy range limits what we can learn from them, so we have excluded them from our analysis in order to focus on LMXBs. A thorough study of supersoft sources in less distant galaxies has recently been conducted by Di Stefano & Kong (2002).

Since the number of greater than 10^{39} ergs s^{-1} sources is small, it is important to check whether there could be significant contamination from background AGNs at these flux levels, especially considering the apparent change in source colors across the 10^{39} ergs s^{-1} threshold. In Table 2, we compare the number of sources in each galaxy with fluxes corresponding to luminosities of $(1–2) \times 10^{39}$ ergs s^{-1} and

[3] See http://cxc.harvard.edu/cal/Links/Acis/acis/Cal_prods/qeDeg/index.html for a complete description.

[4] See http://www.astro.psu.edu/users/chartas/xcontdir/xcont.html.

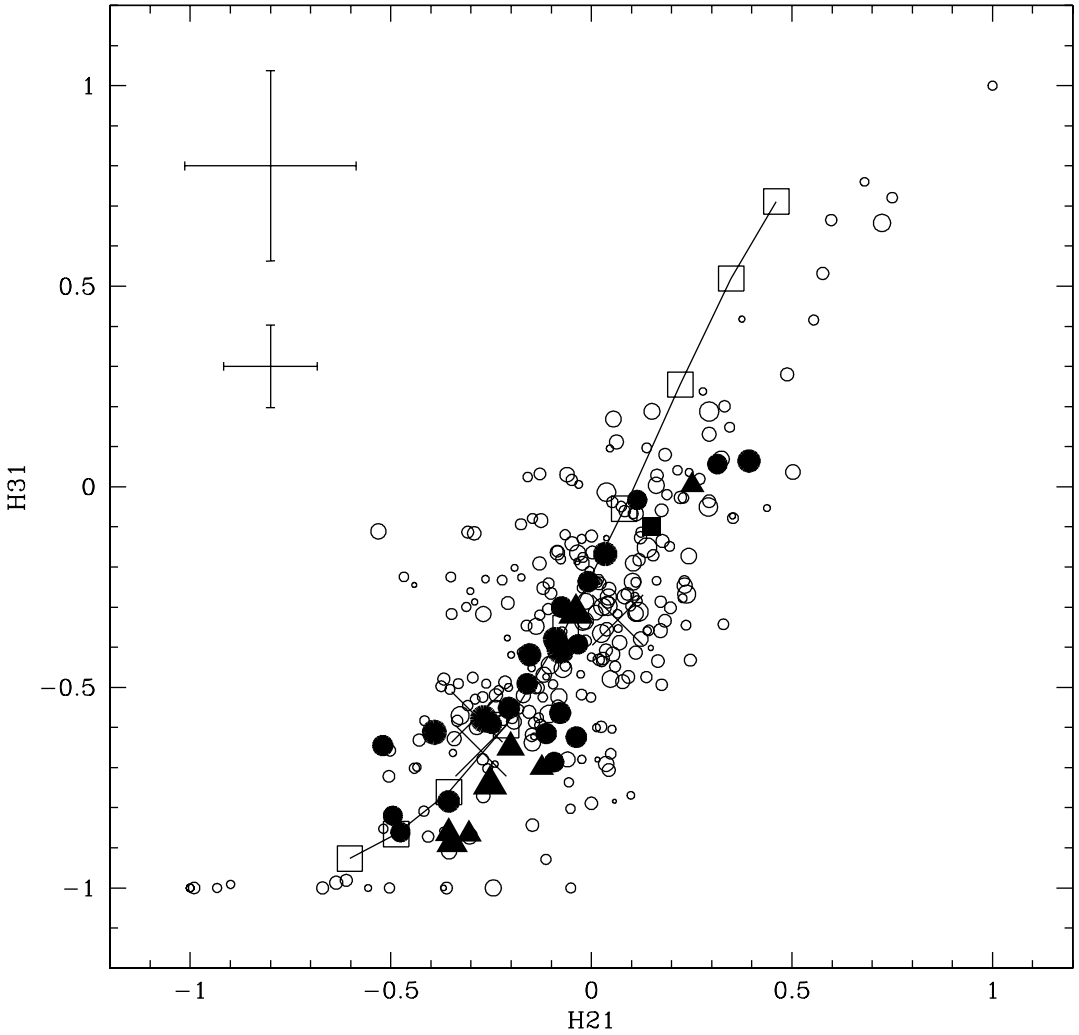

FIG. 2.—X-ray hardness ratios of point sources within NGC 1291, NGC 1316, NGC 1399, NGC 1549, NGC 1553, NGC 4374, NGC 4472, NGC 4494, NGC 46 36, NGC 4649, and NGC 4697. The area of the circle is proportional to the X-ray luminosity of the source. Filled circles represent sources with luminosities of $(1–2) \times 10^{39}$ ergs s^{-1}, and open circles represent sources less luminous than 10^{39} ergs s^{-1}. Filled triangles represent sources that would have luminosities greater than 2×10^{39} ergs s^{-1} if they were at the distance of the galaxies, although they are most likely bright background/foreground objects. Known AGNs are symbolized by large crosses. The colors predicted from a typical ULX spectrum ($kT_{\rm in} = 1.5$ keV) are represented by a filled square. To eliminate scatter, only sources with at least 30 counts were included. Error bars for a 50 count source and a 100 count source (typical of $>10^{39}$ ergs s^{-1} sources) are shown in the upper left. The open squares represent the colors predicted from an absorbed power-law model with an exponent $\Gamma = 0$ (*upper right*) to $\Gamma = 3.2$ in increments of 0.4. [*See the electronic edition of the Journal for a color version of this figure.*]

greater than 2×10^{39} ergs s^{-1} to the number of foreground/background sources expected over the area covered, both for each galaxy and for all the galaxies combined. We have calculated the expected number of foreground/background sources using the 0.5–2.0 keV $\log N - \log S$ relations of both Mushotzky et al. (2000; hereafter M00) and Giacconi et al. (2001; hereafter G01) and extrapolating to a 0.5–6.0 keV *Chandra* count flux using the spectral model assumed in each paper. These two *Chandra* deep field studies predict somewhat different numbers of high-flux sources, as illustrated in Figure 2 of Giacconi et al. (2001). This is most likely the result of small number statistics of the number of sources at the high-flux end of the distribution. We have excluded NGC 1407 from the combined results because of the uncertainty in its distance, which greatly affects the number of high-luminosity sources it contains (see § 3.2). We have also excluded the two spiral bulges, NGC 1291 and M31, for which no luminous sources were detected. For sources with inferred luminosities between 1 and 2×10^{39} ergs s^{-1}, there are 4–5 times more sources than expected from foreground/background sources, so clearly a majority of these sources belong to the galaxies in our sample. Conversely, the 10 sources with inferred luminosities greater than 2×10^{39} ergs s^{-1} are what is expected from foreground/background sources. We note that two of the 10 sources are known to be contained within globular clusters of NGC 1399 (Angelini et al. 2001). The remaining eight sources are what is expected if the M00 and G01 predictions are averaged. The colors of these sources tend to be quite soft and are denoted by filled triangles in Figure 2. This is in accordance with the G01 finding that the bright sources in their deep field had softer spectra than the faint sources.

3.1. *Composite X-Ray Spectrum for Sources with* $L_{\rm X} < 10^{39}$ ergs s^{-1}

Given the tendency of the most luminous sources to be softer than the lower luminosity sources, we have

TABLE 2
NUMBER OF SOURCES DETECTED VERSUS NUMBER EXPECTED FROM BACKGROUND AGNS

	10^{39} ergs s^{-1} < L_X < 2×10^{39} ergs s^{-1}			$L_X > 2 \times 10^{39}$ ergs s^{-1}		
	Number Expected			Number Expected		
Galaxy	M00	G01	Number Detected	M00	G01	Number Detected
NGC 1316.....	1.1	0.8	6	1.7	1.0	1
NGC 1399.....	0.3	0.2	5	0.5	0.3	3
NGC 1407[a]	1.5	1.3	7	2.3	1.6	5
NGC 1407[b]	0.7	0.6	2	1.2	0.7	0
NGC 1549.....	0.4	0.3	2	0.6	0.4	0
NGC 1553.....	0.6	0.4	1	0.9	0.5	1
NGC 3115.....	0.2	0.1	0	0.3	0.2	0
NGC 3585.....	0.3	0.3	1	0.5	0.3	0
NGC 4374.....	0.4	0.3	0	0.7	0.4	1
NGC 4472.....	0.9	0.7	3	1.4	0.8	0
NGC 4494.....	0.2	0.2	1	0.4	0.2	1
NGC 4636.....	0.7	0.5	0	1.1	0.7	2
NGC 4649.....	0.6	0.5	6	1.0	0.6	1
NGC 4697.....	0.5	0.3	1	0.8	0.4	0
Total[c]	6.2	4.7	26	9.9	5.8	10[d]
0–1 r_{eff}	1.0	0.7	10	1.5	0.9	1
1–3 r_{eff}	5.2	4.0	16	8.4	4.9	9[d]

[a] Assuming a distance $d = 28.8$ Mpc.
[b] Assuming a distance $d = 17.6$ Mpc.
[c] Excluding NGC 1407.
[d] Includes two sources known to reside in globular clusters of NGC 1399 and two known AGNs.

redetermined the best-fit power-law exponent for the spectrum of all the sources in each galaxy excluding the sources whose luminosities exceeded 10^{39} ergs s^{-1} as well as the supersoft sources. The results are shown in Figure 3. Upon removal of the most luminous sources, the spectra of the remaining sources appear remarkably uniform from galaxy to galaxy. The unweighted mean and standard deviation of the sample was $\Gamma = 1.56 \pm 0.08$. We performed a simultaneous fit to the 15 data sets within XSPEC, allowing the normalizations for each galaxy to vary while having one common power-law exponent. The best-fit exponent was $\Gamma = 1.56 \pm 0.02$ (90% confidence level), with $\chi^2_\nu = 1.08$ for 903 degrees of freedom. A thermal bremsstrahlung model led to a slightly worse fit (χ^2_ν of 1.14) with $kT_{brem} = 7.3 \pm 0.3$ keV. A disk blackbody model led to a statistically unacceptable fit ($\chi^2_\nu = 1.79$).

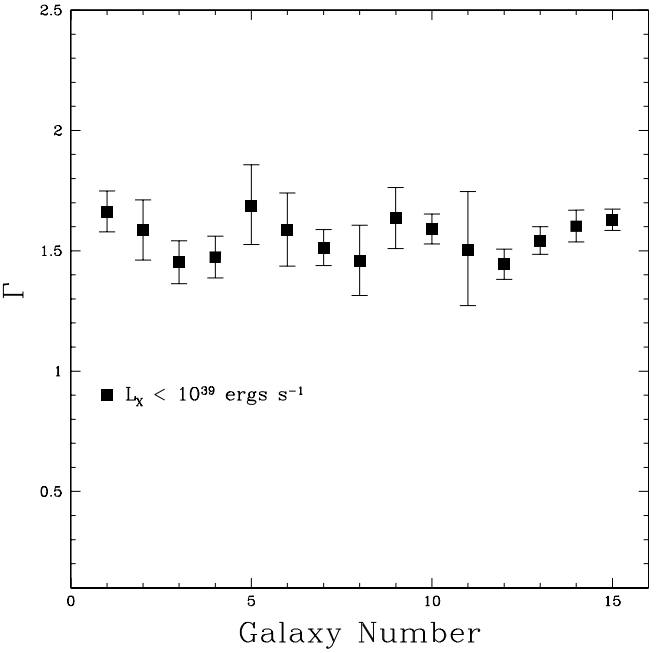

FIG. 3.—Same as Fig. 1 but excluding all sources with luminosities greater than 10^{39} ergs s^{-1}. The spectral properties of the lower luminosity sources are remarkably similar among galaxies.

3.2. *Dependence of LMXB Spectral Properties on Source Luminosity*

We further subdivided the sources into four luminosity classes for each galaxy: (1) $L_X = (1–2) \times 10^{39}$ ergs s^{-1}, (2) 10^{38} ergs s^{-1} < L_X < 10^{39} ergs s^{-1}, (3) 10^{37} ergs s^{-1} < L_X < 10^{38} ergs s^{-1}, and (4) $L_X < 10^{37}$ ergs s^{-1}. Only the bulge of M31 is close enough to contribute to the final class. For the most luminous class, only NGC 1316, NGC 1399, and NGC 4649 are used, since these are the only galaxies where there is clearly an excess of sources over that expected from foreground/background sources. Figure 4 shows the best-fit power-law exponents for the three lower luminosity classes for each galaxy. There was no statistical difference between classes (2) and (3). Interestingly, the spectrum of the lowest luminosity sources ($L_X < 10^{37}$ ergs s^{-1} from the bulge of M31) is indistinguishable from sources in the 10^{37}–10^{39} ergs s^{-1} regime. Thus, on average it appears that the bulk spectral characteristics of LMXBs are the same over at least 3 orders of magnitude in luminosity up to 10^{39} ergs s^{-1}.

The situation is quite different for sources with luminosities of $(1–2) \times 10^{39}$ ergs s^{-1}, as alluded to earlier. Since several galaxies contained only one or two such high-flux sources, a single contaminating background AGN could alter the best-fit power-law index significantly if

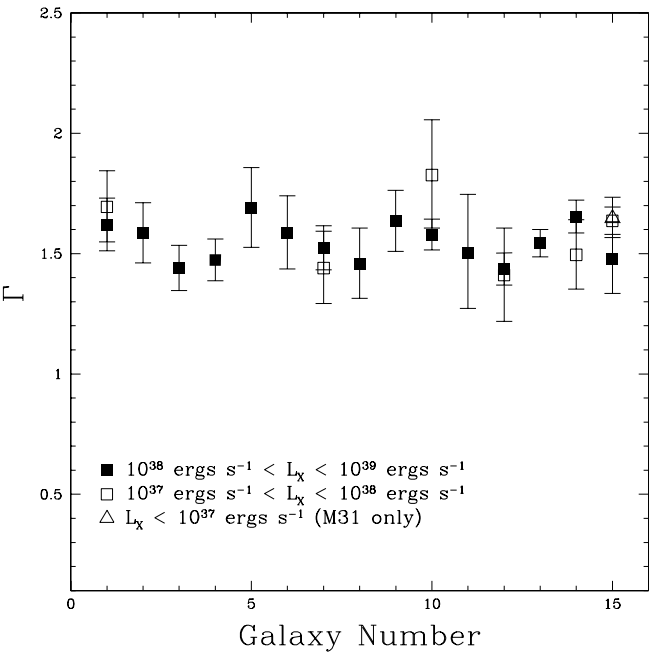

FIG. 4.—Best-fit power-law exponents for each galaxy for three luminosity classes below 10^{39} ergs s^{-1}.

misidentified as an X-ray source within the target galaxy. We have checked to see whether any of the luminous sources coincided spatially with known AGNs. The only high-flux sources in both NGC 4374 and NGC 4697 are known AGNs and have been excluded. NGC 4636 and NGC 4649 each have a bright source that is coincident with optical identifications from the USNO-A2.0 optical catalog (Monet et al. 1998). The $B-R$ value given in the USNO-A2.0 optical for the source in NGC 4649 is -0.7, far too blue to be a globular cluster of NGC 4649, and it is most likely an AGN. The bright source in NGC 4636 has $B-R = 1.7$, which would make it red enough to be a globular cluster. However, such an identification is premature, since a known AGN near NGC 4374 has a similar red color. Given the uncertainty in determining which high-luminosity sources were actually AGNs, we have calculated power-law indices for only galaxies that contained at least four such sources (see Table 3). NGC 1316, NGC 1399, and NGC 4649 all have power-law indices significantly higher than the lower luminosity sources, as the color information of Figure 2 implied. NGC 1407 has a low power-law index ($\Gamma = 1.37 \pm 0.19$) despite containing seven high-luminosity sources, but there is considerable uncertainty in the distance to this galaxy. While we have assumed the Tonry et al. (2001) surface brightness fluctuation distance of 28.8 Mpc, the globular cluster luminosity function distance method gives a distance of only 17.6 Mpc (Perrett et al. 1997). With this smaller distance, only two of the sources would have a luminosity exceeding 10^{39} ergs s^{-1}, with $\Gamma = 1.75 \pm 0.21$, which is more similar to the values obtained for NGC 1316, NGC 1399, and NGC 4649. Also using this distance, the seven sources that yielded $\Gamma = 1.37 \pm 0.19$ would all have luminosities less than 10^{39} ergs s^{-1}, and the low value of Γ would be consistent with that expected from lower luminosity sources in other galaxies. The spectra of the LMXBs in NGC 1407 would at least tentatively argue in favor of the lower distance estimate to this galaxy.

If we make a simultaneous fit for all the galaxies that have at least four high-luminosity sources (and also exclude NGC 1407 because of the uncertainty in its distance) so that the effects of including an unidentified AGN are minimized, we find a best-fit power-law exponent of $\Gamma = 1.96 \pm 0.08$. A summary of the best-fit power laws by luminosity class above and below 10^{39} ergs s^{-1} for each galaxy is given in Table 3, and a summary of the simultaneous fits by luminosity class is given in Table 4.

Although it has been postulated that the break in the luminosity function at $\sim 3 \times 10^{38}$ ergs s^{-1} represents a transition between neutron star and black hole LMXBs, there is no apparent difference in spectral characteristics of sources above and below the break (excluding the very luminous $>10^{39}$ ergs s^{-1} sources). Fitting the spectra of all sources in all the galaxies with luminosities less than 3×10^{38} ergs s^{-1} yielded a best-fit power-law spectrum with $\Gamma = 1.58 \pm 0.03$, while fitting sources more luminous than 3×10^{38} ergs s^{-1} (but less than 10^{39} ergs s^{-1}) yielded $\Gamma = 1.54 \pm 0.03$. This is expected given that differences in the spectral signatures

TABLE 3
SUMMARY OF POWER-LAW SPECTRAL PROPERTIES FOR EACH GALAXY BY LUMINOSITY CLASS

Number	Galaxy	All Sources (Γ)	χ^2_ν/dof	$<10^{39}$ ergs s^{-1} (Γ)	χ^2_ν/dof	(1–2) $\times 10^{39}$ ergs s^{-1} (Γ)	χ^2_ν/dof
1	NGC 1291	$1.66^{+0.09}_{-0.08}$	1.27/49	$1.66^{+0.09}_{-0.08}$	1.27/49	...	...
2	NGC 1316	$1.86^{+0.12}_{-0.11}$	0.71/41	$1.59^{+0.13}_{-0.12}$	0.69/26	$1.86^{+0.28}_{-0.26}$	1.58/13
3	NGC 1399	$1.72^{+0.06}_{-0.06}$	0.94/126	$1.45^{+0.09}_{-0.09}$	1.08/58	$1.95^{+0.14}_{-0.14}$	0.66/25
4	NGC 1407	$1.56^{+0.06}_{-0.06}$	1.41/85	$1.47^{+0.09}_{-0.09}$	1.08/58	$1.37^{+0.19}_{-0.19}$	0.97/14
5	NGC 1549	$1.61^{+0.16}_{-0.16}$	0.56/17	$1.69^{+0.17}_{-0.16}$	0.65/13	...	...
6	NGC 1553	$1.69^{+0.11}_{-0.11}$	1.33/31	$1.59^{+0.15}_{-0.15}$	1.28/23	...	...
7	NGC 3115	$1.59^{+0.07}_{-0.07}$	1.06/61	$1.51^{+0.08}_{-0.07}$	1.07/56	...	...
8	NGC 3585	$1.43^{+0.15}_{-0.15}$	1.32/18	$1.46^{+0.15}_{-0.15}$	1.87/16	...	...
9	NGC 4374	$1.89^{+0.08}_{-0.08}$	0.84/66	$1.64^{+0.12}_{-0.13}$	0.83/32	...	...
10	NGC 4472	$1.57^{+0.06}_{-0.06}$	0.98/116	$1.59^{+0.06}_{-0.06}$	0.96/107	...	...
11	NGC 4494	$1.87^{+0.17}_{-0.16}$	0.82/19	$1.50^{+0.25}_{-0.23}$	0.86/8	...	...
12	NGC 4636	$1.57^{+0.05}_{-0.05}$	0.97/105	$1.44^{+0.06}_{-0.06}$	0.84/88	...	...
13	NGC 4649	$1.61^{+0.04}_{-0.04}$	1.17/122	$1.54^{+0.06}_{-0.06}$	1.30/105	$1.77^{+0.12}_{-0.12}$	1.26/26
14	NGC 4697	$1.63^{+0.06}_{-0.06}$	1.40/80	$1.60^{+0.07}_{-0.07}$	1.23/73	...	...
15	M31	$1.63^{+0.04}_{-0.04}$	1.18/133	$1.63^{+0.04}_{-0.04}$	1.18/133	...	...

TABLE 4
Summary of Simultaneous Power-Law Spectral Fits

Category	Γ	χ^2_ν/dof
All sources, all galaxies	$1.64^{+0.02}_{-0.02}$	1.15/1083
$L_X = (1–2) \times 10^{39}$ ergs s^{-1}	$1.96^{+0.08}_{-0.08}$	1.15/70
$L_X < 10^{39}$ ergs s^{-1}	$1.56^{+0.02}_{-0.02}$	1.08/903
10^{38} ergs s^{-1} $< L_X < 10^{39}$ ergs s^{-1}	$1.56^{+0.02}_{-0.03}$	1.04/727
10^{37} ergs s^{-1} $< L_X < 10^{38}$ ergs s^{-1}	$1.61^{+0.05}_{-0.05}$	1.10/189
$L_X < 10^{37}$ ergs s^{-1} (M31 bulge only)	$1.64^{+0.06}_{-0.06}$	1.32/92
Sources $< 1r_{\rm eff}$	$1.48^{+0.04}_{-0.04}$	1.13/320
Sources 1–2 $r_{\rm eff}$	$1.51^{+0.03}_{-0.04}$	0.94/299
Sources 2–3 $r_{\rm eff}$	$1.53^{+0.06}_{-0.06}$	1.03/134

between black holes in their nonflaring state and neutron stars occur appreciably only at hard X-ray energies ($\gtrsim$5 keV). A disk blackbody model provided a poor fit ($\chi^2_\nu > 1.5$) for both luminosity classes.

3.3. *Globular Cluster versus Non–Globular Cluster Sources*

We have tested whether the spectral properties of LMXBs that reside within globular clusters differ from those not residing within globular clusters. For NGC 1399 and NGC 4472, we used the globular cluster X-ray source identifications of Angelini et al. (2001) and Kundu et al. (2002), respectively, to derive best-fit power laws for LMXBs residing inside and outside of globular clusters. We excluded sources with luminosities that exceeded 10^{39} ergs s^{-1}. For NGC 1399, globular cluster LMXBs had a best-fit power-law index of $\Gamma = 1.33 \pm 0.17$, while for non–globular cluster LMXBs, $\Gamma = 1.62 \pm 0.34$. A similar exercise for NGC 4472 found $\Gamma = 1.51 \pm 0.13$ for globular cluster sources and $\Gamma = 1.57 \pm 0.06$ for non–globular cluster sources. A similar result was found for this galaxy by Maccarone, Kundu, & Zepf (2003). Thus, within the uncertainties, there is no difference in the spectral properties of LMXBs based on their location inside or outside a globular cluster.

3.4. *Radial Dependence of the Spectral Properties of LMXBs*

We also investigated the radial dependence of the spectral properties of LMXBs. Sources were extracted from within 0–1, 1–2, and 2–3 effective radii (again the highest luminosity and supersoft sources were excluded), and a best-fit power-law exponent was obtained. For each radial bin, the spectra from all the galaxies were fitted simultaneously as described above (the spiral bulges of NGC 1291 and M31 were excluded from the fit). For the three radial bins, the best-fit exponents were $\Gamma = 1.48 \pm 0.05$, $\Gamma = 1.51 \pm 0.05$, and $\Gamma = 1.62 \pm 0.06$ (90% uncertainties), respectively. Although the first two radial bins are consistent with one another, the first and third bins are marginally inconsistent. We investigated whether this was due to contamination from unrelated foreground/background sources in the third radial bin. For each galaxy, we used the *Chandra* deep field source count rate of M00 to estimate the expected number of serendipitous sources in the third radial bin. If the number of expected contaminating sources exceeded 30% of the total number of sources actually detected in this radial bin, we excluded it from the simultaneous fit. After excluding NGC 1316, NGC 1553, NGC 4472, NGC 4494, and NGC 4697 because of this criterion, the best-fit power-law exponent from a simultaneous fit of the remaining eight galaxies was $\Gamma = 1.53 \pm 0.06$, which lessens the difference with the inner two radial bins. Thus, there appears to be no radial dependence of the spectral properties of LMXBs at least out to three effective radii. This information is summarized in Table 4.

Given that five of the galaxies had significant contamination in the third radial bin, we redetermined the best-fit power-law exponent for all sources with $L_X < 10^{39}$ ergs s^{-1} sources without including sources in the third radial bin. However, the results before and after the exclusion were consistent within the uncertainties. In addition, the composite spectrum was not changed significantly.

4. DISCUSSION

4.1. *Comparison with Previous Studies*

The constraints on the bulk spectral properties of LMXBs of $\Gamma = 1.56 \pm 0.02$ (or alternatively $kT_{\rm brem} = 7.3 \pm 0.3$ keV) represent the tightest constraints derived to date. Previously, Matsumoto et al. (1997) simultaneously fitted the spectra of several early-type galaxies observed with *ASCA* with a two-component model to fit jointly the hot gas and LMXB components; the best-fit power-law model yielded $\Gamma = 1.8 \pm 0.4$. More recently, White (2002) also used *ASCA* data for six early-type galaxies to set a constraint of $\Gamma = 1.83^{+0.10}_{-0.11}$ (90% confidence limits) on the power-law index, in marginal disagreement with our result (although their best-fit bremsstrahlung temperature of $kT_{\rm brem} = 6.3^{+1.6}_{-1.1}$ is consistent with our value). However, since the rather poor spatial resolution of *ASCA* could not in general resolve most of the sources, the more luminous sources undoubtedly biased the power-law exponent higher, owing to the soft spectral nature of these luminous sources. If we make a composite fit to the spectra from all 15 galaxies without excluding the most luminous sources, we obtain $\Gamma = 1.64 \pm 0.02$, in closer agreement with the White (2002) result. Furthermore, three of the galaxies in our sample have $\Gamma \sim 1.9$ (Fig. 1). If these three galaxies had been part of a smaller sample than what we have compiled here, we would have obtained an average value closer to $\Gamma = 1.8$ for the sample.

4.2. *High/Soft versus Low/Hard Spectral States?*

The result that sources with luminosities of $(1–2) \times 10^{39}$ ergs s^{-1} are substantially softer on average than sources less luminous than 10^{39} ergs s^{-1} is highly reminiscent of the high-flux/soft spectral state versus low-flux/hard spectral shape behavior exhibited by Galactic black hole X-ray binary candidates (e.g., Tanaka & Lewin 1995; Nowak 1995). While in their low/hard state, the spectra of Galactic black hole X-ray binaries are characterized by a power law with $\Gamma = 1.3–1.7$ with an exponential cutoff at about 100 keV, while in their high/soft state, they exhibit a disk blackbody component ($kT_{\rm in} \sim 1$ keV) plus a power-law component with $\Gamma \sim 2.5$. While the high-energy cutoff of the low/hard state is obviously impossible to detect in our sample, our best-fit power law of $\Gamma = 1.56 \pm 0.02$ for sources with $L_X < 10^{39}$ ergs s^{-1} is certainly consistent with Galactic examples in their low/hard state. Intriguingly, if we fit simultaneously the most luminous sources in our sample with a disk blackbody plus power-law model, we get best-fit values of $kT_{\rm in} = 1.76^{+0.16}_{-0.23}$ keV and $\Gamma = 2.61^{+0.51}_{-0.40}$,

with the power-law component contributing between 25% and 68% of the total 1–10 keV luminosity from galaxy to galaxy. This ratio is that expected from black hole binaries in the very high state of Figure 1 of Nowak (1995), in which the binaries are accreting close to the Eddington limit. This spectral model was also a better fit than the single power-law model ($\chi^2_\nu = 0.89/66$ degrees of freedom [dof] versus $\chi^2_\nu = 1.15/70$ dof).

Finally, it is unlikely that the luminous sources found in elliptical and S0 galaxies are actually multiple lower luminosity sources. If this were the case, one would not expect the difference in spectral characteristics between these sources and lower luminosity sources. A single accreting object provides the most reasonable explanation.

4.3. *Spatial Distribution of the Luminous Sources*

The spatial distribution of the luminous sources can yield useful insight into the nature of these sources. We have determined how many greater than 10^{39} ergs s^{-1} sources are found between 0 and 1 $r_{\rm eff}$ and 1 and 3 $r_{\rm eff}$, respectively, for all 13 elliptical and S0 galaxies in our sample collectively. Since these sources typically have 100 or more X-ray counts, the effects of missing sources because of the degradation of the point-spread function with increasing off-axis distance or from contamination from high X-ray surface brightness hot gas in some of the galaxies are minimized and can be safely ignored.

If the sources are distributed randomly over the field of view of the ACIS detector, we would expect 8 times more sources in the 1–3 $r_{\rm eff}$ bin than in the 0–1 $r_{\rm eff}$ bin. Because the 3 $r_{\rm eff}$ radius contour did not always fit onto the ACIS chip for the larger galaxies, the ratio for our sample is expected to be about 5.5 : 1 rather than 8 : 1. Conversely, if the sources follow the optical light, one would expect about half as many sources within the 1–3 $r_{\rm eff}$ bin as in the 0–1 $r_{\rm eff}$ bin.

For the greater than 2×10^{39} ergs s^{-1} sources, once the two sources known to be associated with globular clusters of NGC 1399 are removed, there are seven sources in the 1–3 $r_{\rm eff}$ bin and only one within one effective radius (Table 2). This is consistent with the sources being randomly distributed over the detector, providing further evidence that these sources are unrelated foreground/background sources. The spatial distribution of the $(1\text{–}2) \times 10^{39}$ ergs s^{-1} sources is clearly not random. Once an estimate for the foreground/background sources is removed, there are about nine sources within 1 $r_{\rm eff}$ and 11 sources within 1–3 $r_{\rm eff}$. Thus, the spatial distribution of these sources is much flatter than the optical light, in which there should have been twice the number of sources in the inner spatial bin than in the outer one. This is not unexpected, given that a large percentage of the sources are within globular clusters and that the spatial distribution of globular clusters within early-type galaxies is known to be significantly flatter than the optical light, which follows a de Vaucouleurs profile. In fact, the two high-luminosity sources within both NGC 1399 and NGC 4472 that fall within the *Chandra–Hubble Space Telescope* overlap region of the galaxies reside within globular clusters. Further optical work will be required to determine whether all the high-luminosity sources reside within globular clusters, but the extended spatial distribution of the sources would suggest that they do.

4.4. *Are the Luminous Sources Ultraluminous X-Ray Sources?*

The existence of very luminous off-center X-ray point sources in spiral galaxies has been the subject of considerable interest in recent years (e.g., Makishima et al. 2000; Roberts & Warwick 2000; King et al. 2001). Usually found in star-forming regions of spiral arms and having $L_{\rm X} > 10^{39}$ ergs s^{-1} (although this lower limit on the luminosity is somewhat arbitrary), the nature of these ultraluminous X-ray sources (ULXs) has been difficult to explain. Although a few ULXs appear to be supernovae that detonated in a very dense environment (Fabian & Terlevich 1996; Immler, Pietsch, & Aschenbach 1998; Blair, Fesen, & Schlegel 2001), significant temporal variability has ruled out this possibility in many other cases, strongly indicating that they are some form of accreting X-ray binary. However, ULXs in NGC 1313, M81, and IC 342 do not exhibit the typical high/soft–low/hard flux/spectral behavior that black hole binaries exhibit but instead show a reverse behavior (Makishima et al. 2000; Mizuno, Kubota, & Makishima 2001). Still, the fact that ULX spectra can be adequately fitted with a disk blackbody model argues that they are an accreting binary of some kind.

The high X-ray luminosities of the more luminous ULXs imply that the mass of the central accreting object must exceed 50 $M_\odot$ if they are accreting at the Eddington limit (where $L_{\rm Edd} = 1.3 \times 10^{38}$ ergs s$^{-1} M/M_\odot$ and M is the mass of the accreting object), assuming the emission is unbeamed. Sub-Eddington accretion rates typical of Galactic X-ray binaries would imply an even higher black hole mass. Such a class of intermediate-mass black holes would provide the crucial missing link between stellar mass ($\lesssim 10\ M_\odot$) black holes and supermassive ($>10^6\ M_\odot$) black holes at the centers of galaxies. However, black holes of this size are very difficult to create from the collapse of single stars, given that current stellar evolution models predict that massive main-sequence progenitor stars will lose too much mass via stellar winds throughout the course of their lifetime to retain a greater than 50 $M_\odot$ core to produce such a massive black hole. This has created some skepticism of the intermediate-mass black hole explanation. Alternatively, the X-ray emission might not be isotropic but instead beamed at us. King et al. (2001) has proposed that the most likely candidate in a beaming scenario is a period of thermal timescale mass transfer in binaries with intermediate- or high-mass donor stars, which naturally explains the presence of the ULXs in regions of recent star formation.

While the focus of ULX studies has been on sources in spiral galaxies, information gathered on possible ULXs in elliptical galaxies has yet to be incorporated into their explanation. A substantial number of high-luminosity X-ray sources in early-type galaxies was found by Colbert & Ptak (2002) in a survey with the *ROSAT* HRI, although the lack of spectral resolution of that instrument did not allow for a spectral comparison of these sources to ULXs in spiral galaxies.

From our *Chandra* sample, we find that very luminous ($>2 \times 10^{39}$ ergs s^{-1}) sources are absent from elliptical and S0 galaxies, save for two luminous sources within globular clusters of NGC 1399. Furthermore, the sources in our sample with luminosities of $(1\text{–}2) \times 10^{39}$ ergs s^{-1} have different spectra than ULXs in spiral galaxies. A

single disk blackbody model does not provide a good fit to the composite spectrum of the high-luminosity sources within NGC 1316, NGC 1399, and NGC 4649 (χ^2_ν of 2.74 for 70 dof) unlike spiral galaxy ULXs (e.g., Makishima et al. 2000). The addition of a power-law tail is required at very high significance, something required for only one ULX studied to date (M33 X-8; Makishima et al. 2000). The disk blackbody + power-law model required to fit the high-luminosity sources (§ 4.2) is much more similar to the model used to fit high-state black hole binaries than the model used to fit ULXs. This is illustrated in Figure 2, where the colors predicted from a disk blackbody with an inner temperature of $kT_{\rm in} = 1.5$ keV (*filled square*) are significantly different from the colors of the high-luminosity sources.

The two very luminous ($\sim 4 \times 10^{39}$ ergs s^{-1}) sources found within globular clusters of NGC 1399 by Angelini et al. (2001) appear to be very rare objects indeed. It is unlikely that any other such high-luminosity sources exist in our sample given that the number of expected serendipitous foreground/background objects should account for all the other high-flux sources in our sample, statistically speaking, although further optical work will be needed to search for possible optical counterparts of the very luminous sources. If such rare, very luminous sources are specific to globular clusters, then perhaps it is not surprising that both are found within globular clusters of NGC 1399 given that NGC 1399 has such a large number of globular clusters (it has a globular cluster specific frequency that is 2–3 times that of typical elliptical galaxies; Harris 1991).

The combined spectra of the two globular cluster sources also look more like those of a high-state black hole binary than a ULX. A disk blackbody alone provided a very poor fit to the data (χ^2_ν of 2.48 for 32 dof), while a simple power law provided a very good fit with $\Gamma = 1.93 \pm 0.11$, very similar to the best-fit power-law exponent for the $(1–2) \times 10^{39}$ ergs s^{-1} sources, although in this instance the addition of a disk blackbody model to the power law did not significantly improve the fit. Thus, it is possible that these very luminous sources are not ULXs (although they have ULX-like luminosities) and represent a different type of accreting object from that responsible for ULXs in spiral galaxies.

One possibility for these very luminous globular cluster sources is accretion onto a central intermediate-mass black hole at the center of the globular cluster. The formation of luminous X-ray sources within globular clusters has been discussed in detail by Miller & Hamilton (2002). In their scenario, a $\gtrsim 50\ M_\odot$ black hole sinks to the center of the globular cluster and accretes smaller black holes over the lifetime of the cluster to grow to a mass of $\sim 1000\ M_\odot$. The creation of the initial 50 $M_\odot$ black hole (the smallest mass black hole that would not be ejected from the cluster by recoil during three-body interactions) might not be a problem in the low-metallicity environment of a globular cluster, since mass-loss rates of very massive stars are predicted to be mild to negligible for low-metallicity stars (see, e.g., Vink, de Koter, & Lamers 2001). If the accretion efficiency of such a black hole was 0.01–0.1 as in Galactic black holes, X-ray luminosities of 10^{39}–10^{40} ergs s^{-1} could be achieved. Such a scenario alleviates the problem of having the black hole emit persistently near its Eddington limit.

If the well-known relation in elliptical galaxies and spiral bulges between the stellar velocity dispersion and mass of the central black hole (e.g., Gebhardt et al. 2000a) is extrapolated down to objects the size of globular clusters, the relation predicts that globular clusters will contain central black holes with masses on the order of $10^3\ M_\odot$. In fact, kinematical evidence for a 2500 $M_\odot$ black hole in the center of the Galactic globular cluster M15 (Gebhardt et al. 2000b) indicates that globular clusters are indeed capable of harboring intermediate-mass black holes. Although the lack of a very luminous X-ray source at the center of M15 indicates that the black hole is not currently being fed, the presence of very luminous X-ray sources in globular clusters might serve as an indication that central massive black holes are a common feature of stellar systems over a wide range of masses ranging from giant galaxies to globular clusters. Demonstrating that the ULX is at the dynamical center of the globular cluster, however, is not currently feasible even for the nearest early-type galaxies.

In summary, it does not appear that elliptical galaxies contain ULXs, at least not the kind found within spiral galaxies. For sources below 2×10^{39} ergs s^{-1}, the implied masses assuming the sources are accreting near their Eddington limit are only $\lesssim 15\ M_\odot$, which does not contradict the current estimates of the upper mass limit of stellar mass black holes. Furthermore, their X-ray spectra are substantially different from those of ULXs in spiral galaxies, as Figure 2 indicates. Their spectral similarities to known black hole binaries strongly argues that these sources are simply black holes accreting near their Eddington limit and do not require either beaming or an intermediate-mass black hole to explain their existence. In addition, the only two sources with luminosities exceeding 2×10^{39} ergs s^{-1} that are conclusively in the galaxies of our sample (and probably the only two) also have much different spectra from ULXs. The increasing evidence that globular clusters can contain intermediate-mass black holes also provides a method for explaining their high X-ray luminosities that is problematic for spiral galaxy ULXs that occur in the field.

4.5. *Implications for the Hot Gas Component*

The uniformity of the spectral properties of LMXBs with luminosities below 10^{39} ergs s^{-1} has useful implications for the study of hot gas in early-type galaxies. First, in galaxies where most of the LMXB emission is not resolved (either galaxies observed with *XMM-Newton* or more distant galaxies where excessively long *Chandra* observations would be needed to detect sources fainter than $\sim 10^{38}$ ergs s^{-1}), the LMXB component will contribute significantly to the diffuse emission, particularly for galaxies that are not rich in hot gas. In this case, the ability to fix the spectral shape of the LMXB component ($\Gamma = 1.56$ or $kT_{\rm brem} = 7.3$ keV) will allow tighter constraints to be placed on the temperature and especially the metallicity of the hot gas. All that is required is that LMXBs more luminous than 10^{39} ergs s^{-1} be removed from the spectrum. As an example of this, we have extracted the spectrum of the diffuse emission from within one effective radius of the X-ray–faint galaxy NGC 3115 and fitted the emission with a MEKAL component (Mewe, Gronenschild, & van den Oord 1985; Kaastra & Mewe 1993; Liedahl, Osterheld, & Goldstein 1995) to model the hot gas component and a power law to model the unresolved LMXB component. If the power-law exponent is left as a free parameter, a gas temperature of $kT_{\rm MEKAL} = 0.61^{+0.28}_{-0.31}$ is obtained, and the metallicity of the gas is

unconstrained. After fixing the power-law component at $\Gamma = 1.56$, the temperature is constrained significantly better, with $kT_{\rm MEKAL} = 0.61^{+0.16}_{-0.18}$. In addition, the metallicity of the gas could now be constrained to be less than 5% of the solar value.

Second, the result that LMXBs in the bulge of M31 with luminosities as low as 10^{36} ergs s^{-1} have bulk spectral characteristics that are indistinguishable from more luminous LMXBs will greatly simplify the determination of the total gaseous X-ray luminosity, $L_{\rm X,gas}$, in very X-ray faint galaxies. In these types of galaxies, where very low X-ray count rates will not allow the gas and LMXB components to be separated spectrally as in NGC 3115, $L_{\rm X,gas}$ can be very difficult to determine accurately. A small error in the estimation of the unresolved LMXB component would lead to a large error in the derived luminosity of the gaseous component. Although such an error would have a negligible effect on the determination of $L_{\rm X,gas}$ in well-known, gas-rich galaxies such as NGC 4636 and NGC 1399 (where the gaseous emission is over an order of magnitude more luminous than the LMXB component), this will not be the case for a galaxy such as NGC 3585. If we assume that all the diffuse counts in NGC 3585 above 2 keV are from unresolved LMXBs (since the emission from 0.3 keV gas typical of such X-ray–faint galaxies would be negligible above 2 keV), we can convert the 2–6 keV flux to the 0.3–6 keV flux that emanates from unresolved sources and subtract this amount from the total diffuse amount to yield the gaseous flux. If we use a $\Gamma = 1.56$ power-law model in the conversion, we find that 60% of the 0.3–6 keV diffuse flux is from unresolved LMXBs, leaving 40% for the hot gas component. Conversely, if we assume a $\Gamma = 1.9$ power-law model, LMXBs account for 83% of the diffuse emission, leaving only 17% of the diffuse emission for the gas component. Clearly, the derivation of $L_{\rm X,gas}$ is highly dependent on our choice of Γ for the unresolved sources, and factors of 2 or more uncertainties can arise. Knowing that we can safely use a value of $\Gamma = 1.56$ will significantly decrease the uncertainty in $L_{\rm X,gas}$ for these very X-ray faint systems.

Determining $L_{\rm X,gas}$ accurately for X-ray–faint galaxies is particularly important in deriving the $L_{\rm X,gas}$ versus $L_{\rm opt}$ relation, which has been used extensively to characterize the hydrodynamic history of gas lost from stars within the galaxy over the lifetime of the galaxy (Canizares, Fabbiano, & Trinchieri 1987; Davis & White 1996; Brown & Bregman 1998). Comparison of the X-ray to optical luminosities of galaxies found $L_{\rm X,gas} \propto L_B^{1.7-3.0}$ among the various studies. The rather large spread in the best-fit exponent is in large part due to uncertainties in the luminosity of the lower X-ray luminosity systems and how each investigator chose to subtract off the LMXB component. Future studies with *Chandra* will minimize the uncertainty in the $L_{\rm X,gas}$ values and lead to a more accurate determination of the exponent.

5. CONCLUSIONS

We have used *Chandra* data for 15 early-type systems to constrain the spectral and spatial properties of LMXBs in these galaxies. We have found that once the most luminous ($>10^{39}$ ergs s^{-1}) sources are removed from the combined spectra of the sources, the spectra of the sum of the sources have very similar values among the galaxies. When all the galaxies are fitted simultaneously with a power-law spectral model, the best-fit power-law exponent is $\Gamma = 1.56 \pm 0.02$. Even faint sources as dim as 10^{36} ergs s^{-1} in the bulge of M31 have similar spectral properties to the more luminous sources. There was no apparent difference in the spectral properties of LMXBs as a function of galactic radius. Nor was there a significant difference in the spectral properties of sources based on their presence within or outside a globular cluster.

A significant number of sources with luminosities of $(1–2) \times 10^{39}$ ergs s^{-1} were found within the galaxies, and they exhibited significantly softer spectral properties than the fainter sources. The disk blackbody + power-law model used to model their spectra is very reminiscent of Galactic black hole X-ray binaries when they are in their very high state. Their spectra were also quite different from ULXs found within spiral galaxies. The simplest explanation of these sources is that they are $\sim$7–15 $M_\odot$ accreting near their Eddington limit. The spatial distribution of these sources is significantly more extended than the optical light.

With rare exception, sources more luminous than 2×10^{39} ergs s^{-1} are absent from early-type galaxies. The number and spatial distribution of the sources with fluxes corresponding to 2×10^{39} ergs s^{-1} or greater if they are at the distance of the galaxy is consistent with them being unrelated background/foreground sources. The only exceptions to this seem to be two $\sim 4 \times 10^{39}$ ergs s^{-1} sources found within globular clusters of NGC 1399. Their spectra are also quite different from that of a typical spiral galaxy ULX. Their presence within a globular cluster suggests that globular clusters might harbor intermediate-mass black holes that are accreting at a few percent of their Eddington limit.

Finally, we have discussed how these constraints on the spectral properties of LMXBs, especially the fainter ones, can lead to better constraints on the luminosity, temperature, and metallicity of the hot gas within early-type galaxies that contain little gas.

We thank the referee, Alexis Finoguenov, for many useful comments that improved the quality of the manuscript. J. A. I. was supported by *Chandra* Fellowship grant PF9-10009, awarded through the *Chandra* Science Center. J. N. B. acknowledges support from NASA grants GO0-1148 and GO1-2087. The *Chandra* Science Center is operated by the Smithsonian Astrophysical Observatory for NASA under contract NAS8-39073.

REFERENCES

Angelini, L., Loewenstein, M., & Mushotzky, R. F. 2001, ApJ, 557, L35
Bauer, F. E., Brandt, W. N., Sambruna, R. M., Chartas, G., Garmire, G. P., Kaspi, S., & Netzer, H. 2001, AJ, 122, 182
Blair, W. P., Fesen, R. A., & Schlegel, E. M. 2001, AJ, 121, 1497
Blanton, E. L., Sarazin, C. L., & Irwin, J. A. 2001, ApJ, 552, 106
Brown, B. A., & Bregman, J. N. 1998, ApJ, 495, L75
Canizares, C. R., Fabbiano, G., & Trinchieri, G. 1987, ApJ, 312, 503
Caon, N., Capaccioli, M., & D'Onofrio, M. 1994, A&AS, 106, 199
Capaccioli, M., Held, E. V., & Nieto, J.-L. 1987, AJ, 94, 1519
Colbert, E. J. M., & Ptak, A. F. 2002, ApJS, 143, 25
Davis, D. S., & White, R. E., III. 1996, ApJ, 470, L35
de Vaucouleurs, G. 1975, ApJS, 29, 193
Dickey, J. M., & Lockman, F. J. 1990, ARA&A, 28, 215
Di Stefano, R., & Kong, A. K. H. 2002, ApJ, submitted
Fabian, A. C., & Terlevich, R. 1996, MNRAS, 280, L5
Finoguenov, A., & Jones, C. 2002, ApJ, 574, 754
Gebhardt, K., Pryor, C., O'Connell, R. D., Williams, T. B., & Hesser, J. E. 2000a, AJ, 119, 1268

Gebhardt, K., et al. 2000b, ApJ, 539, L13
Giacconi, R., et al. 2001, ApJ, 551, 624 (G01)
Goudfrooij, P., Hansen, L., Jorgensen, H. E., Norgaard-Nielsen, H. U., de Jong, T., & van den Hoek, L. B. 1994, A&AS, 104, 179
Harris, W. E. 1991, ARA&A, 29, 543
Immler, S., Pietsch, W., & Aschenbach, B. 1998, A&A, 331, 601
Irwin, J. A., Sarazin, C. L., & Bregman, J. N. 2002, ApJ, 570, 152
Jorgensen, I., Franx, M., & Kjaergaard, P. 1995, MNRAS, 276, 1341
Kaastra, J. S., & Mewe, R. 1993, A&AS, 97, 443
Kim, D.-W., & Fabbiano, G. 2003, ApJ, in press (astro-ph/0206369)
King, A. R., Davies, M. B., Ward, M. J., Fabbiano, G., & Elvis, M. 2001, ApJ, 552, L109
Kormendy, J. 1984, ApJ, 286, 132
Kraft, R. P., Kregenow, J. M., Forman, W. R., Jones, C., & Murray, S. S. 2001, ApJ, 560, 675
Kundu, A., Maccarone, T., & Zepf, S. 2002, ApJ, 574, L5
Liedahl, D. A., Osterheld, A. L., & Goldstein, W. H. 1995, ApJ, 438, L115
Maccarone, T., Kundu, A., & Zepf, S. 2003, ApJ, in press (astro-ph/0210143)
Makishima, K., et al. 2000, ApJ, 535, 632
Matsumoto, H., Koyama, K., Awaki, H., Tsuru, T., Loewenstein, M., & Matsushita, K. 1997, ApJ, 482, 133
Mewe, R., Gronenschild, E. H. B. M., & van den Oord, G. H. J. 1985, A&AS, 62, 197
Miller, M. C., & Hamilton, D. P. 2002, MNRAS, 330, 232
Mizuno, T., Kubota, A., & Makishima, K. 2001, ApJ, 554, 1282
Monet, D., et al. 1998, USNO-A2.0: A Catalog of Astrometric Standards (Washington, DC: USNO)
Mushotzky, R. F., Cowie, L. L., Barger, A. J., & Arnaud, K. A. 2000, Nature, 404, 459 (M00)
Nowak, M. 1995, PASP, 107, 1207
Peletier, R. F., Davies, R. L., Illingworth, G. D., Davis, L. E., & Cawson, M. 1990, AJ, 100, 1091
Perrett, K. M., Hanes, D. A., Butterworth, S. T., Kavelaars, J. J., Geisler, D., & Harris, W. E. 1997, AJ, 113, 895
Randall, S. W., Sarazin, C. L., & Irwin, J. A. 2002, ApJ, submitted
Roberts, T. P., & Warwick, R. S. 2000, MNRAS, 315, 98
Ryden, B. S., Forbes, D. A., & Terlevich, A. I. 2001, MNRAS, 326, 1141
Sarazin, C. L., Irwin, J. A., & Bregman, J. N. 2000, ApJ, 544, L101
———. 2001, ApJ, 556, 533
Soria, R., & Wu, K. 2002, A&A, 384, 99
Swartz, D. A., Ghosh, K. K., Suleimanov, V., Tennant, A. F., & Wu, K. 2002, ApJ, submitted (astro-ph/0203487)
Tanaka, Y., & Lewin, W. H. G. 1995, in X-Ray Binaries, ed. W. H. G. Lewin, J. van Paradijs, & E. P. J. van den Heuvel (Cambridge: Cambridge Univ. Press), 126
Tonry, J. L., Dressler, A., Blakeslee, J. P., Ajhar, E. A., Fletcher, A. B., Luppino, G. A., Metzger, M. R., & Moore, C. B. 2001, ApJ, 546, 681
van den Bergh, S. 2000, The Galaxies of the Local Group (Cambridge: Cambridge Univ. Press)
van den Heuvel, E. P. J., Bhattacharya, D., Nomoto, K., & Rappaport, S. A. 1992, A&A, 262, 97
Vink, J. S., de Koter, A., & Lamers, H. J. G. L. M. 2001, A&A, 369, 574
White, R. E., III. 2002, in ASP Conf. Ser. 262, The X-Ray Universe at Sharp Focus, ed. E. Schlegel, & S. Vrtilek, (San Francisco: ASP), 153